Determination of mixing layer height from ceilometer backscatter profiles

Marijn de Haij*, Wiel Wauben, Henk Klein Baltink
Royal Netherlands Meteorological Institute, P.O. Box 201, 3730 AE De Bilt, The Netherlands

ABSTRACT

Mixing layer height (MLH) is a key parameter in many atmospheric boundary layer studies and processes. A Wavelet method is developed for the automatic determination of mixing layer height from backscatter profiles of an LD-40 ceilometer. Furthermore, a quality flag is introduced to identify unreliable MLH detections. The performance of the Wavelet MLH algorithm is analysed by comparing the results with MLH estimates from radiosondes, wind profiler and research lidar measurements. A correlation coefficient of 0.64 is found between ceilometer and radiosonde determinations when using only ceilometer MLH detections with good quality. A statistical analysis of the ceilometer MLH for a six year data set shows satisfactory results for availability and the results show the main characteristics of MLH, i.e. the diurnal and seasonal cycle. However, problems arise e.g. in case of multiple (well defined) aerosol layers, which renders the selection of the correct mixing layer top ambiguous. Furthermore, in spring and summer the detection of the MLH for deep (convective) boundary layer often fails. This is mostly due to the high variability of the aerosol backscatter signal with height which limits the range for MLH estimation in those conditions.

Keywords: ceilometer, lidar, aerosol, boundary layer, mixing layer height

1. INTRODUCTION

In this paper an assessment is made of the determination of mixing layer height (MLH) from backscatter profiles of the Vaisala-Impulsphysik LD-40 ceilometer. This instrument is operated by KNMI at about 20 locations in the meteorological measurement network in The Netherlands. If the determination of the MLH is feasible, this network could provide a useful monitoring tool for the spatial variation of MLH on a national scale. By collocation with scintillometry instruments during a measurement campaign, the spatial variation of the MLH can be coupled directly to a variation in the sensible heat flux, which is the driving mechanism behind the development of the daytime mixing layer. These results can be applied e.g. for assessment and improvement of boundary layer parameterizations of (mesoscale) atmospheric models or inverse modeling of greenhouse gases on a national scale (Hutjes, 2005). Mixing layer height has been estimated from various in situ and remote sensing observations during the past decades. A comprehensive overview of the most commonly used measurement platforms and their advantages and disadvantages is presented in Fischer et al. (1998).

A ceilometer transmits laser pulses and measures the backscattered signal. The strength of the backscattered signal depends on the amount of scattering particles at a certain altitude. The time interval between transmission and reception of the signal determines the corresponding altitude. The presence of aerosols can be detected in the backscatter profiles of ceilometers. Aerosols are mainly emitted at the surface and the concentration of aerosol is therefore generally higher in the atmospheric boundary layer than in the free atmosphere. Therefore, the MLH estimation from lidar systems is based on the detection of the sharp decrease in aerosol backscatter at the top of the mixing layer. This negative gradient marks the interface between the aerosol containing mixing layer and the relatively clean free atmosphere. Furthermore, a maximum in the time variance of the backscatter is often found at the top of the mixing layer. This is related to the dynamic behavior of the air at the mixing layer top and the associated strong exchange of air originating from the free atmosphere with air from the mixing layer throughout the entrainment zone. Two major classes of MLH determination from lidar backscatter profiles exist: 1) based on the direct analysis of backscatter gradient and/or variance (e.g. De Ruiter, 1991; Menut et al., 1999; Schäfer et al., 2004) and 2) based on the application of a wavelet transform for the detection of the (negative) gradient in the backscatter profile.

* haijde@knmi.nl; phone +31 30 2206 774; fax +31 30 2210 407; http://www.knmi.nl

Remote Sensing of Clouds and the Atmosphere XI, edited by James R. Slusser, Klaus Schäfer, Adolfo Comerón,
Proc. of SPIE Vol. 6362, 63620R, (2006) · 0277-786X/06/$15 · doi: 10.1117/12.691050

Wavelet transforms are commonly used in recent studies for MLH determination from lidar observations (e.g. Cohn and Angevine, 2000; Davis et al., 2000; Brooks, 2003). The most important advantage of wavelet methods is the decomposition of the signal in both altitude as well as vertical spatial scale of the structures in the backscatter signal. Cohn and Angevine (2000) found a good agreement between estimates of MLH and the entrainment zone thickness (EZT) by two lidars and a wind profiling radar (correlation coefficients of 0.87 and 0.95 for the MLH estimates). It was shown that the (Haar) wavelet transform is a powerful tool to detect a significant decrease in aerosol backscatter, even at very high time resolution. Vertical averaging of the profile, like for the application of gradient/variance methods, does not seem necessary because of the implicit averaging when applying the wavelet transform. Davis et al. (2000) applied wavelet analysis to airborne infrared lidar data to obtain an objective determination of boundaries in aerosol backscatter that are associated with the boundary layer structure. The dilation (width of the wavelet) corresponding with the maximum in wavelet variance, was used for the determination of these boundaries. The method was adapted for cases with a lot of noise in the backscatter signal. Brooks (2003) carried out an extensive theoretical analysis of the method in order to study the MLH determination from backscatter profiles that deviate from the ideal situation, e.g. with a sloping background or a deep inversion. It was found that the method produces dilation-dependent errors in the MLH determination. An alternative method was developed using multiple dilations. The Wavelet MLH algorithm developed here combines features of the algorithms described above.

Conditions, like fog, boundary layer clouds, precipitation or advected aerosol layers, caused problems in the determination of MLH in all studies concerning this subject. In these situations, it is very hard to distinguish unambiguously between the top of the mixing layer and the other features in the backscatter profile that also show a strong gradient signature.

2. LD-40 CEILOMETER

The Vaisala-Impulsphysik LD-40 ceilometer (Impulphysik, 1998) makes use of the LIDAR principle. The measured backscatter profile as a function of height is the result of multiple laser emissions. Typically, 65000 pulses are emitted every 15 seconds. The backscatter profile provides information on the amount of particles that cause the backscatter, as a function of height. The LD-40 has a measurement range of 25 to 43000 ft (7.5 m to 13.6 km) and operates at a resolution of 25 ft (7.5 m). It uses laser diodes with 855 nm wavelength that are pulsed at a frequency of 6494 Hz. The pulse energy power is 1 μJ and pulse duration is 50 ns.

The LD-40 is a bi-axial system, hence the beams of the transmitter and receiver do not overlap completely in the lowest 1125 m. This is a disadvantage with respect to a single lens system, like e.g. the CT25K ceilometer. Up to 60 m the overlap is zero. Between 60 and 1125 m, the overlap increases to 1. The backscatter signal measured in this range has to be corrected for the incomplete overlap between transmit and receiver beam (Münkel and Räsänen, 2004). The backscatter profiles are corrected with a standard overlap table as provided by Vaisala.

Backscatter profiles are reported by the LD-40 every 15 seconds, together with the lowest three cloud bases (C1, C2 and C3), vertical visibility (VV), maximum range of detection (CX) and a precipitation index (PI). These additional parameters are derived from the backscatter profile by the internal LD-40 software (Impulsphysik, 1999). The backscatter data in the LD-40 KNMI format are coded as the natural logarithm of the measured power P in pW, multiplied with the squared height r in m: $\ln(Pr^2)$. The backscatter resolution is 0.2 (expressed in $\ln(Pr^2)$) and values range from 10.1 to 22.7.

3. METHODOLOGY

3.1 Data preprocessing

When applying the MLH detection algorithm, only that part of the backscatter signal with a sufficiently high signal-to-noise-ratio (SNR) should be taken into account. When regions of low SNR values are considered, the MLH determination might get contaminated due to backscatter structures related to noise instead of atmospheric signals. For this purpose, a LD-40 data preprocessing procedure that was introduced within the Cloudnet project (Haeffelin, 2005; personal communication) is used. This procedure ignores any points of the backscatter profile that have a SNR below a prescribed value. The representative value for noise is computed from the signal in the upper 3 km of the backscatter profile. The height at which the transition to data points with SNR<1 occurs, is used as the SNR stop level h_{SNR}. The SNR stop level is the level above which the MLH algorithm is not applied anymore.

Backscatter signals from other origin than aerosol are filtered out before the MLH algorithm is applied. The parameters derived by the internal Vaisala algorithm (see section 2) are used to detect the occurrence of these disturbances. Firstly, the MLH algorithm is not applied if the precipitation index PI exceeds a value of 3 (light precipitation). Furthermore, the vertical domain on which the algorithm is applied is constrained by the SNR stop level, but also by the first cloud base C1, the vertical visibility VV and the maximum range of detection CX. The minimum values of these latter three parameters within the MLH processing interval of 10 minutes are the values used in the filter. For PI, the maximum value within a 10 minute interval is considered.

3.2 The Wavelet MLH algorithm

The Wavelet algorithm is applied to the 10 minute averaged range and overlap corrected backscatter profile within a vertical domain of 90 – 3000 m. This 10 minutes averaged profile is computed from 10 single backscatter profiles. This means that only one out of every four measured profiles is used. For each averaged profile the top of two significant aerosol layers are detected by the Wavelet algorithm. This gives the opportunity to detect the mixing layer height as well as the top of a secondary aerosol layer, like e.g. an advected aerosol layer or the residual layer. Hereafter the two detected layer heights are called MLH1 and MLH2 respectively (De Haij et al., 2006).

The Wavelet MLH method presented here, uses the scale averaged power spectrum profile $\overline{W_B}(b)$ of the wavelet transform with 24 dilations between 15 and 360 m and step size 15 m. The step size used is the smallest possible, i.e. 2 range gates. For each range gate up to the upper boundary of the vertical domain (as determined by the lowest value of C1, VV, CX and h_{SNR}) the average value $\overline{W_B}(b)$ is computed from the contributions of each available single dilation for that corresponding height. For increasing dilation, the height level at which $W_B(a,b)$ obtains a value for the first time also increases due to the decreasing vertical range for which the wavelet function is defined. If a wavelet does not fit due to its dilation size, the contribution of this dilation is omitted in the calculation of the scale averaged power spectrum profile.

The top of the first layer, MLH1, is detected at the first range gate at which the scale averaged power spectrum $\overline{W_B}(b)$ shows a local maximum, exceeding a threshold value of 0.1. This threshold value is empirically chosen, based on the analysis of several cases with both well pronounced and less clearly pronounced mixing layer tops. MLH2 is optionally determined in the height range between MLH1 and the upper boundary of detection. A valid MLH2 is detected at the level with the strongest local maximum of $\overline{W_B}(b)$ provided that this maximum is larger than the $\overline{W_B}(b)$ of MLH1.

3.3 Quality index

A quality index is introduced to distinguish between detections of the top of well-pronounced and more ambiguous mixing layers respectively. The magnitude of the jump in backscatter, centered on the MLH level is used as a measure for the quality of the detection. More specifically, the difference between the averaged backscatter from 150 m below MLH up to the last level below MLH (B_d) and the average backscatter from the first level above MLH up to 150 m above MLH (B_u) is used as a quantity for the quality index (see Table 1).

Table 1. Classification of the quality indices used for mixing layer height detection.

color code	trigger	description
White	No detection of MLH	No MLH detection
Red	$B_d - B_u < 0.25$	Poor MLH detection
Yellow	$0.25 \le B_d - B_u \le 0.50$	Weak MLH detection
Green	$B_d - B_u > 0.50$	Good MLH detection

The threshold values for the different quality index classes are to some extent chosen arbitrarily, and are estimated by assessing cases with transitions between well-pronounced and ambiguous mixing layer heights. A disadvantage of this quality index is that it is independent of the absolute value of the backscatter (in $\ln(Pr^2)$), although smaller variations are

expected at the top of a mixing layer characterized by a lower backscatter signal. Furthermore, the quality index of a MLH with another aerosol layer on top (either advected or residual) or closely below a cloud layer will be significantly suppressed due to the relative high aerosol load that is measured beyond this MLH.

4. RESULTS

4.1 Case studies

In this section some cases are discussed, representing a selection of typical atmospheric conditions included in the data set of the LD-40 ceilometers in De Bilt and the experimental site in Cabauw. Four typical cases are plotted in Figure 1. The legend of the variables shown is listed in Table 2. The occurrence of a 'Poor' MLH1 estimate is represented by a black dot just above the x-axis of each contour plot.

Table 2. Legend of the backscatter contour plots in Figure 1.

———	LD-40 SNR<1 height
•	LD-40 MLH1 Wavelet algorithm
Δ	LD-40 MLH2 Wavelet algorithm
X	LD-40 first cloud base C1
●	Radiosonde MLH Richardson bulk method
▲	Radiosonde MLH Parcel method
▪	RIVM lidar first MLH

The backscatter contour plot and resulting MLH estimates for Cabauw on July 27, 2002 are shown in Figure 1a. The development of a convective mixing layer can clearly be observed, with a sharp and strong decrease in aerosol backscatter between the mixing layer and the free atmosphere, resulting in a MLH time series with low variability between successive points. The build up of the convective layer is disturbed around 1400 UTC by the development of cumulus clouds on top of the mixing layer, which cause a termination of the algorithm at the height of the first cloud base. Around 1730 UTC a new aerosol layer is observed, which extends between 200 and 500 m above ground level during the evening. The occurrence of this layer coincides with a change in wind direction and marks the advection of an air mass containing aerosol from another source area. During the first two and last three hours of this day, the secondary MLH2 is successfully detected on top of an elevated aerosol layer. In this case MLH2 can be associated with the top of the residual layer.

In Figure 1b a completely different situation is presented that occurred at De Bilt on July 19, 2003. Whereas a well defined aerosol layer is observed until approximately 1000 UTC, the MLH estimates in the period thereafter are strongly variable both for MLH1 and MLH2. These poor estimates coincide with a lowered height of the SNR stop level, which is only about 1200 m during the afternoon. In this case the 'correct' MLH is indicated by the radiosonde methods (see Table 2) at 1200 UTC. The radiosonde estimate of the MLH is approximately 2100 m, located near the cloud bases which are detected by the LD-40. There is too much noise in the backscatter signal for the algorithm to be able to detect the correct values of MLH, hence the vertical range for MLH detection is limited by the SNR stop level. The mixing layer is too deep to obtain a reliable backscatter signal for the whole mixing layer given the amount of available aerosol. The 'Poor' quality index is frequently observed for this day, indicating the unreliable character of these MLH detections.

A case with a wintertime shallow mixing layer is shown in Figure 1c, for De Bilt on January 14, 2006. This day, with near-neutral stability at 1200 UTC, is a relatively easy case for the MLH algorithm, as seen in the fairly constant time series of MLH1. The decrease in aerosol backscatter at the top of the mixing layer is evident and sharp. No 'Poor' quality indices are observed. The 1200 UTC radiosonde Parcel method (Van Pul et al., 1994) estimate of MLH however diverges very much with respect to the LD-40 estimates. This is caused by the fact that the Parcel method only gives reliable estimates during convective conditions. Above the shallow mixing layer, with its top roughly between 250 and 400 m during the day, the top of a secondary aerosol layer MLH2 is sometimes detected.

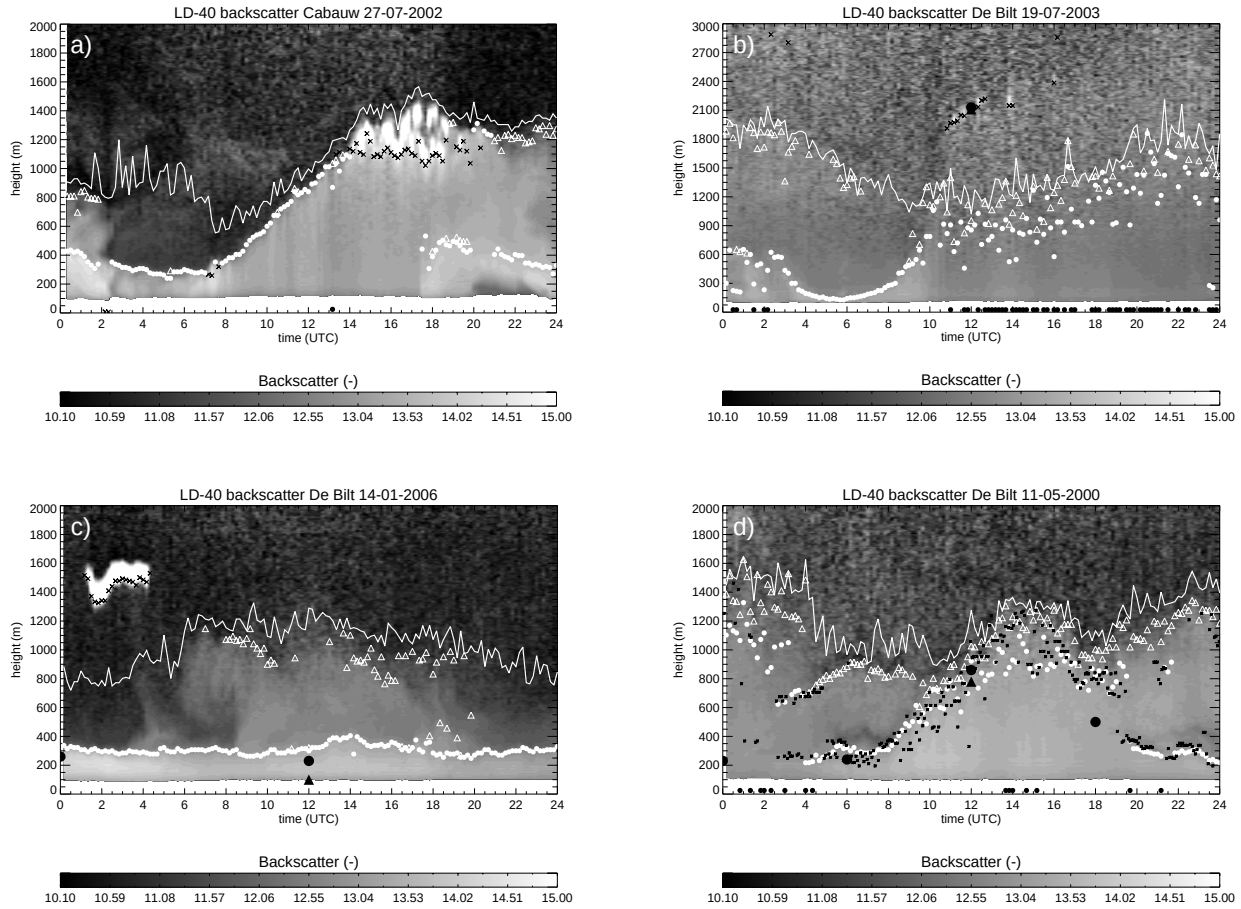

Fig. 1. LD-40 backscatter contour plots with resulting MLH estimates from the Wavelet algorithm: a) Cabauw, July 27, 2002; b) De Bilt, July 19, 2003; c) De Bilt, January 14, 2006; d) De Bilt, May 11, 2000. The legend of the plots is listed in Table 2. Radiosonde MLH estimates below 50 m are omitted.

Backscatter contours and MLH estimates by the ceilometer algorithm and the lowest MLH estimate by the RIVM research lidar (De Ruiter, 1991) are shown in Figure 1d for May 11, 2000. The research lidar was located only 5 kilometers from the LD-40 in De Bilt. The LD-40 and RIVM MLH detections show good agreement at a first glance, but during the period of convective development (roughly between 0800 and 1500 UTC) the temporal variability of the MLH as derived by both instruments is large. The estimates of Wavelet MLH1 are lower than the values of RIVM MLH, especially for the period after noon. Some 'Poor' quality indices are also seen in the figure for this period. The reason for the high variability is probably the large depth of the aerosol backscatter inversion, ranging e.g. between 800 and 1150 m for the backscatter profile 1200 UTC. This causes ambiguity in the detection by the algorithms, resulting in a high temporal variability of MLH estimates. Note that the 0600 UTC and 1200 UTC and – to a lesser extent 1800 UTC – estimates of MLH from the radiosonde Richardson bulk method (Fischer et al., 1998) support the MLH as determined by the LD-40 and RIVM lidar algorithms.

4.2 Algorithm performance analysis

A data set containing six years of backscatter profiles (2000-2005) from the LD-40 at the KNMI test field in De Bilt is used for the assessment of the overall performance of the Wavelet MLH algorithm with respect to the monthly availability and reliability of MLH estimates.

The monthly mean diurnal cycle of the MLH1 and MLH2 heights and the SNR stop level are shown in Figure 2. The expected shape resembling the growth of a convective mixing layer is observed, with an evident annual cycle of the amplitude of the diurnal variation. The smallest amplitude is found for December (110 m), whereas April demonstrates

the maximum amplitude of around 570 m. However, the monthly mean MLH during daytime observed for spring and summer months is lower than expected. This is related to the inability of the algorithm to detect most of the deep mixing layers heights. An example of such a case is De Bilt on July 19, 2003, as discussed in the previous section. The MLH1 growth time (defined as the duration between the occurrence of minimum and maximum height in the MLH1 diurnal cycle) is between 7.2 hours in November and 11.5 hours in July. The SNR stop level shows an inverse-like shape during the day, just like MLH2. This is probably caused by the larger amount of background noise in the backscatter signal during daytime. Furthermore, the occurrence of daytime convective clouds and the coinciding SNR decrease because of extinction of the backscatter signal in these clouds possibly contribute to this shape.

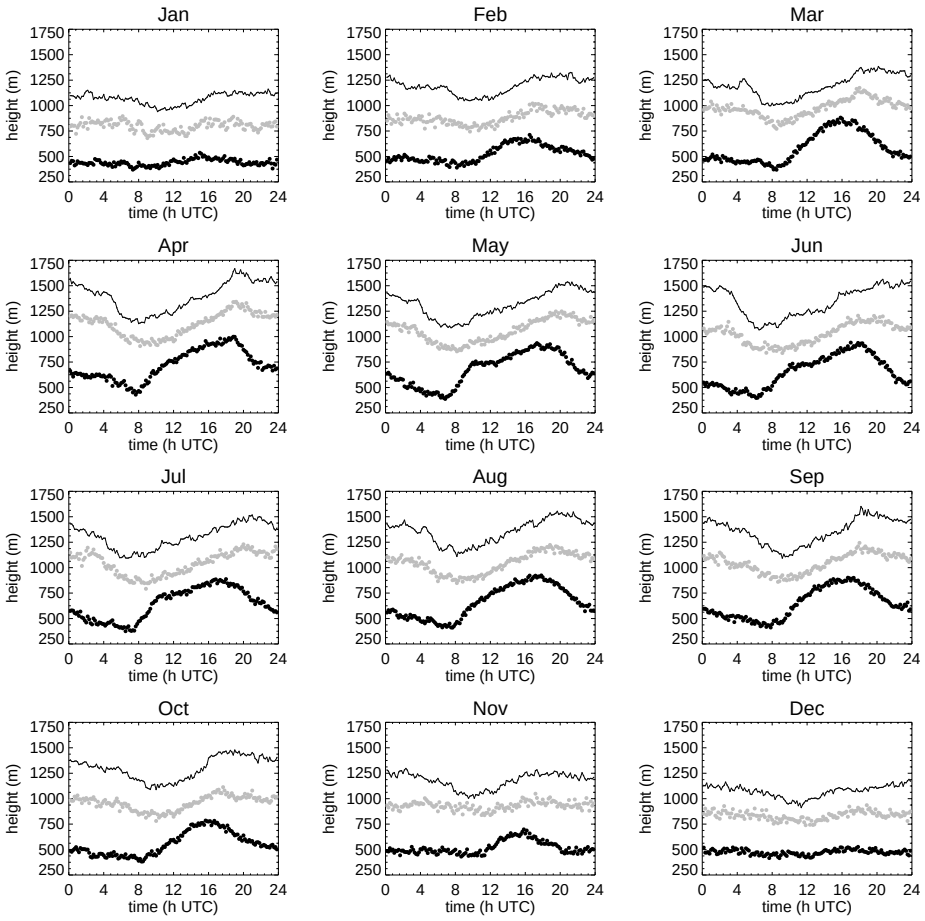

Fig. 2. Monthly mean diurnal cycle of Wavelet MLH1 (black dots), MLH2 (grey dots) and the SNR stop level (black line) for the LD-40 in De Bilt, period 2000-2005.

An overview of the detection rates of the Wavelet MLH1 estimates in the six year period is presented in Figure 3. The results in this table are based on the total number of available backscatter profiles for each month; periods with no data are not included in the analysis. The overall detection rate for MLH1 is between 43 % (January) and 68 % (June), but note that the relative contribution of 'Weak' and 'Poor' detections also increases with increasing detection rate. The most important reason for the lower detection rates during the winter months is the larger amount of weather conditions, like fog, rain and clouds, which inhibit a successful MLH detection. Whereas in January fog, precipitation (PI) and clouds (C1) terminate the algorithm in 3.9 %, 8.5 % and 44.3 % of the total number of cases respectively, in June these percentages are only 0.6 %, 5.0 % and 26.3 %. The maximum contribution of the two lower quality indices together is 44.9 % in April (minimum 15.0 % in January). The higher daytime values of mixing layer height as observed for the spring and summer months in Figure 2 generally coincide with lower quality indices. This is related to the enhanced vertical variability in the backscatter signal and hence the increased chance on a faulty MLH detection on a less pronounced jump in the aerosol backscatter. Note also the large contribution of C1 in the cases filtered out for July with

respect to the surrounding months. This is most likely caused by the very cloudy and precipitative July months in the analysis period 2000-2005. Except for the year 2003, all July months in De Bilt had a precipitation amount and cloud cover above normal conditions.

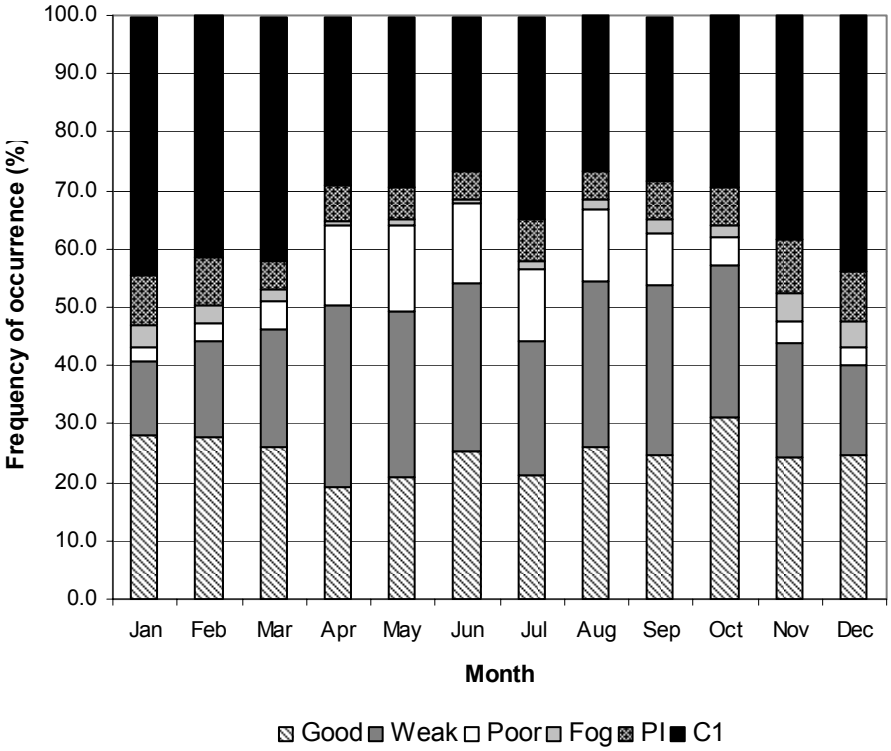

Fig. 3. Monthly mean detection rates for Wavelet MLH1, in De Bilt, period 2000-2005. Successful MLH1 detections are subdivided in the three quality classes: 'Good', 'Weak' and 'Poor'. Terminations of the Wavelet algorithm are ascribed to the cause: 'Fog', 'PI' (precipitation), 'C1' (cloud base).

Figure 4 shows the histograms of the frequency of occurrence of the night (1800-0600 UTC) and daytime (0600-1800 UTC) MLH for June 2000 detected by the LD-40 Wavelet MLH1 and the lowest MLH detected by the RIVM research lidar. The large number of detections in the RIVM histogram is related to the higher detection rate as well as to the higher temporal resolution of the RIVM algorithm. Compared to the histogram of Wavelet MLH1 (Figure 4a), the histogram of the RIVM MLH (Figure 4b) is much more spread out and also shows a significant contribution of higher MLHs. Not only is the amount of detections between 2100 and 3000 m substantially higher (about 6 %), the daytime MLH detections between 1080 and 1500 m also show a striking difference with respect to the LD-40 MLH values. A possible explanation of the high detection rates and shift towards higher MLH in the histogram of the RIVM MLH is the ability of the RIVM algorithm to detect MLH in or beyond cloud layers. Whereas the LD-40 MLH algorithm is terminated if it is not triggered up to the height of the first cloud base, the RIVM algorithm often detects MLH around decreasing backscatter signatures on top of detected cloud bases. For June 2000, 18 % of all RIVM MLH detections is above the estimated RIVM cloud base. However, if a correction is applied for the RIVM MLH estimates above a cloud base, the histogram resembles the LD-40 histogram only slightly better. The cause of the significant differences between the RIVM and LD-40 mixing layer height estimates is still under investigation.

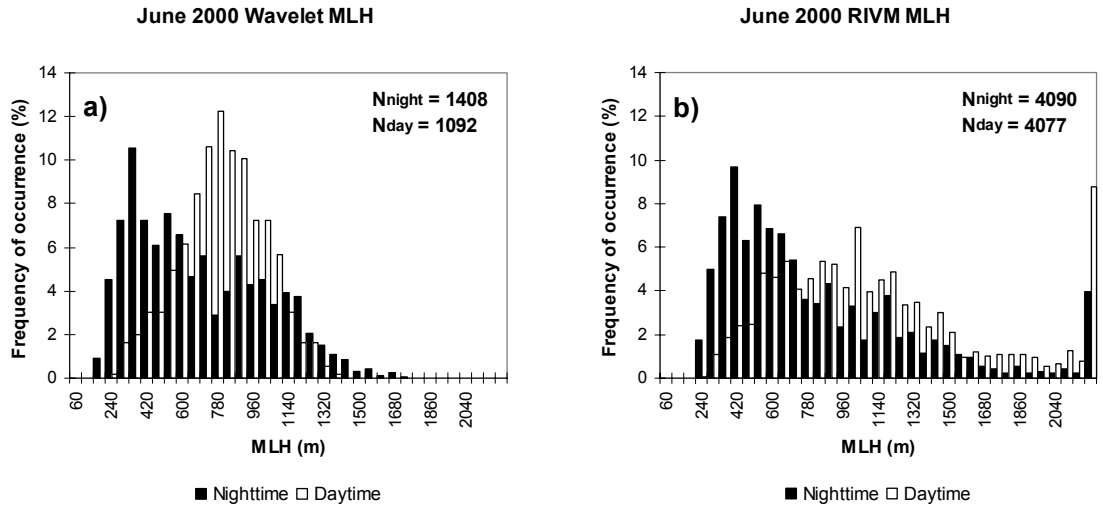

Fig. 4. Histograms of the frequency of occurrence for June 2000 MLH as determined by the a) Wavelet algorithm and b) RIVM algorithm. Detections are subdivided in nighttime (1800-0600 UTC) and daytime (0600-1800 UTC). A bin size of 60 metres is used, the bin on the far right side contains all MLH detections reported higher than 2100 m.

4.3 Comparison with other measurement platforms

A comparison of MLHs estimated by the Wavelet MLH algorithm and the Richardson bulk method applied to 1200 UTC radiosonde profiles in De Bilt, is shown in Figure 5. The same six year period as before is considered, i.e. 2000-2005. The 1200 UTC radiosonde in De Bilt is mostly launched between 1115 and 1130 UTC, so that it passes the 500 hPa level around 1200 UTC. Therefore, the 1140 UTC MLH estimates from the LD-40 are used in this comparison to guarantee a good collocation of measurements in the boundary layer.

From Figure 5a it is clear that the agreement between the two measurement platforms is poor if all MLH estimates are considered. In particular for values of LD-40 MLH above 500 m much scatter is observed. The MLH derived by the radiosonde methods is mostly higher with respect to the LD-40 estimates. Differences up to approximately 1700 m, or 340 % of the original LD-40 MLH are observed in some cases. The correlation coefficient of 0.34 is very low. The comparison with the radiosonde Parcel method (not shown) results in an even lower value for R^2 of 0.27. A major improvement in agreement between the LD-40 and the radiosonde MLH is seen when only the detections with the highest quality index are taken into account (Figure 5b). A lot of the scatter observed in the overall scatter plot has disappeared, resulting in a value for R^2 of 0.64, while the linear fit $y = ax + b$ results in a = 1.24 and b = -45. The detection rate decreases to 18.5 % as a result of the selection of cases with a good quality. An additional rejection of detections for which the Richardson MLH is beyond the SNR stop level (not shown) gives a correlation coefficient of 0.77 with a detection rate of only 16.6 %.

The inability of the LD-40 algorithm to detect the top of deep mixing layers is again illustrated in Figure 6. The time series of monthly mean 1200 UTC mixing layer height as estimated by the LD-40 and radiosonde are shown for De Bilt in the period 2000-2005. The shaded area in the summer and autumn of 2002 coincides with a period during which KNMI did not launch radiosondes frequently. Therefore this period is not considered. The annual cycle in the MLH estimates is clearly visible in all time series shown. Note the evident higher estimates of LD-40 MLH in winter compared to the Parcel method and the underestimation of LD-40 MLH in summer with respect to the MLH determined by the Parcel and Richardson bulk methods. Also note that the value of the mean radiosonde MLH is even beyond the mean SNR stop level for most of the spring and summer months. More specifically, around 18 % of all 1961 cases analysed at 1200 UTC in the period 2000-2005 is affected by the limited vertical range of the LD-40 for MLH estimation. The time series of MLH calculated after rejection of all MLH1 estimates for which the Richardson MLH is beyond the SNR stop level, results in a much better agreement (not shown) although the magnitude of the differences is still significant.

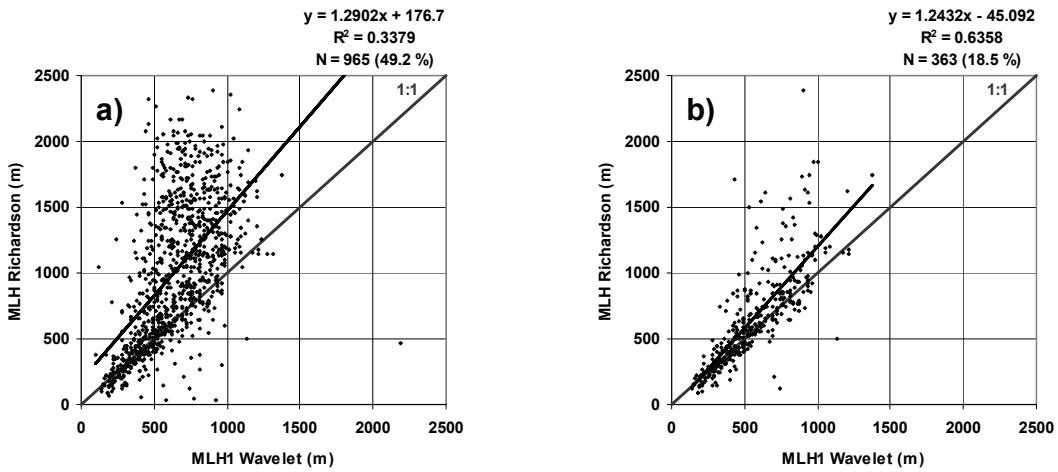

Fig. 5. Scatter plots for LD-40 Wavelet MLH1 vs. radiosonde MLH estimates by the Richardson bulk method, for De Bilt at 1200 UTC, period 2000-2005: a) all simultaneous estimates, b) simultaneous estimates with a 'Good' Wavelet MLH1 quality index.

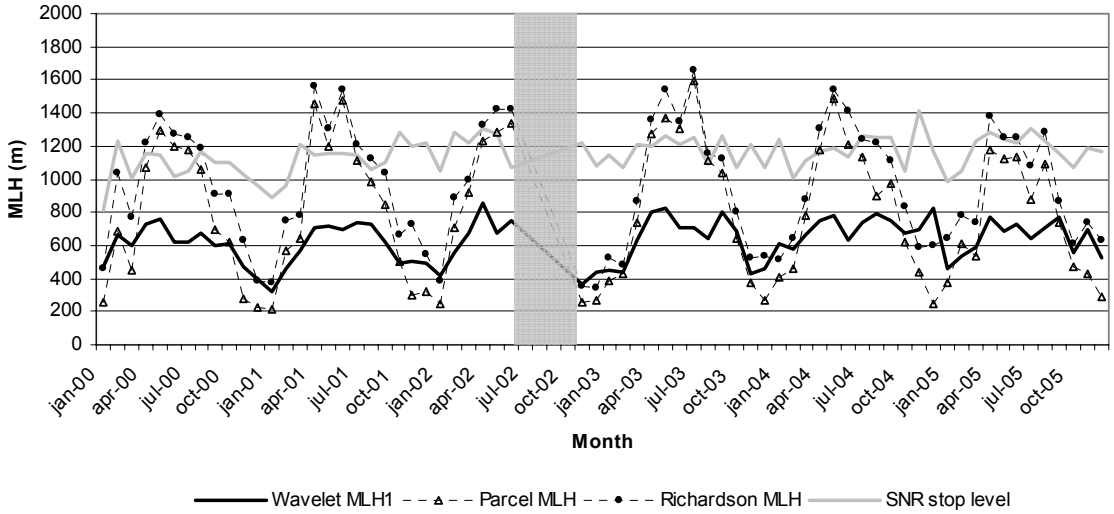

Fig. 6. Monthly mean 1200 UTC time series for coinciding estimates of MLH as derived by the methods LD-40 Wavelet, radiosonde Parcel and radiosonde Richardson bulk, for all simultaneous estimates (N=810).

Eight days in August 2001 were used for the comparison between MLH estimated by LD-40 and the Vaisala LAP-3000 wind profiler in Cabauw. Days were only selected if at least half of the number of wind profiler detections during the period 0700-1600 UTC were present simultaneously with the MLH1 detections. Hence, days with persistent cloud decks were rejected and only days containing a well-defined development of the mixing layer remained in the analysis. The eight days considered here were August 14, 15, 17, 18, 22, 23, 29 and 30.

The scatter plot for all 149 simultaneous detections during these days is shown in Figure 7. Again note the small scatter for low MLHs up to approximately 500 m. The regression coefficients for the l.s.q. linear fit over the entire range are a = 1.05 and b = -30 and the corresponding correlation coefficient is 0.89. If only the LD-40 detections with a 'Good' quality index are taken into account (not shown), the correlation coefficient becomes 0.94.

MLH time series on four of the eight days of the comparison are shown in Figure 8. Note the high consistency of the estimates for low morning MLHs (< 500 m), whereas the higher detections that follow later on the day diverge more. This is possibly a result of the aforementioned variability in the aerosol backscatter signal for increasing height. This causes faulty (lower) detections by the ceilometer MLH algorithm. The LD-40 measurements on August 17 report a

developing cloud layer between 1030 and 1400 UTC, with its cloud base located between approximately 1000 and 1400 m. The coinciding LD-40 MLH is observed roughly 200 m lower than the MLH estimated by the wind profiler and the radiosonde at 1200 UTC. The cloud layer seems to be the direct cause for this disagreement. The MLH detections for the corresponding period are mainly indexed as 'Poor'. Another remarkable feature from Figure 8 is the fluctuating and diverging LD-40 MLH with respect to the wind profiler MLH between 1000 and 1200 UTC on August 22. A pronounced advected aerosol layer confuses the LD-40 algorithms here. The base of this layer sets in near the top of the preceding mixing layer top around 0930 UTC and slowly merges with the developing mixing layer during the following two hours.

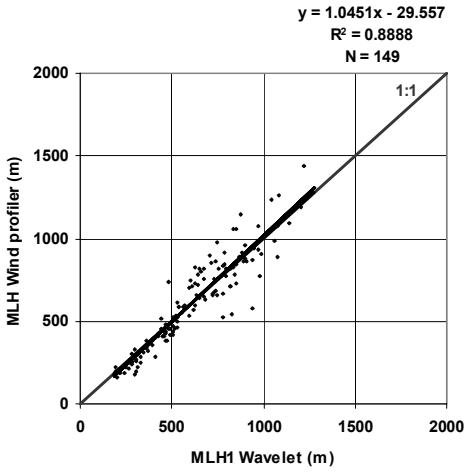

Fig. 7. Scatter plot for LD-40 Wavelet MLH1 vs. wind profiler MLH for eight days in August 2001, in Cabauw. A total of 149 coinciding detections is used.

5. CONCLUSIONS

A wavelet method is developed to derive the mixing layer height from backscatter profiles measured with a Vaisala-Impulsphysik LD-40 ceilometer. The detection of the mixing layer height is based on the (strong) decrease in aerosol backscatter at the transition from mixing layer to the relatively clean free atmosphere. Although the detection is feasible by the method presented, limitations certainly exist. The main findings can be summarized as follows:

- The reliability of the MLH detection is strongly connected to the variability of the aerosol backscatter signal in height in the mixing layer. Profiles that show a fairly constant and sufficient amount of aerosol backscatter result most of the time in a reliable detection of MLH. This mainly occurs when the mixing layer grows not too deep, e.g. in a shallow wintertime mixing layer. Especially in strong convective conditions in spring and summer, the vertical range of MLH detection by the LD-40 is limited.
- A deep inversion layer at the top of the mixing layer can cause a high temporal variability of MLH estimates.
- The afternoon decay of the convective mixing layer forms a problem for LD-40 MLH estimation. The large amount of aerosol in the residual layer on top of the decaying mixing layer, lowers the contrast with the mixing layer and hence decreases the possibility of a correct MLH detection.
- The algorithm has a problem with the detection of very shallow MLHs. This is especially observed during periods with a nocturnal (stable) layer. The problem is probably caused by the lowest detection height of the LD-40 (i.e. 90 m) and perhaps also by the poor numerical resolution and truncation of the backscatter values in the KNMI data format.

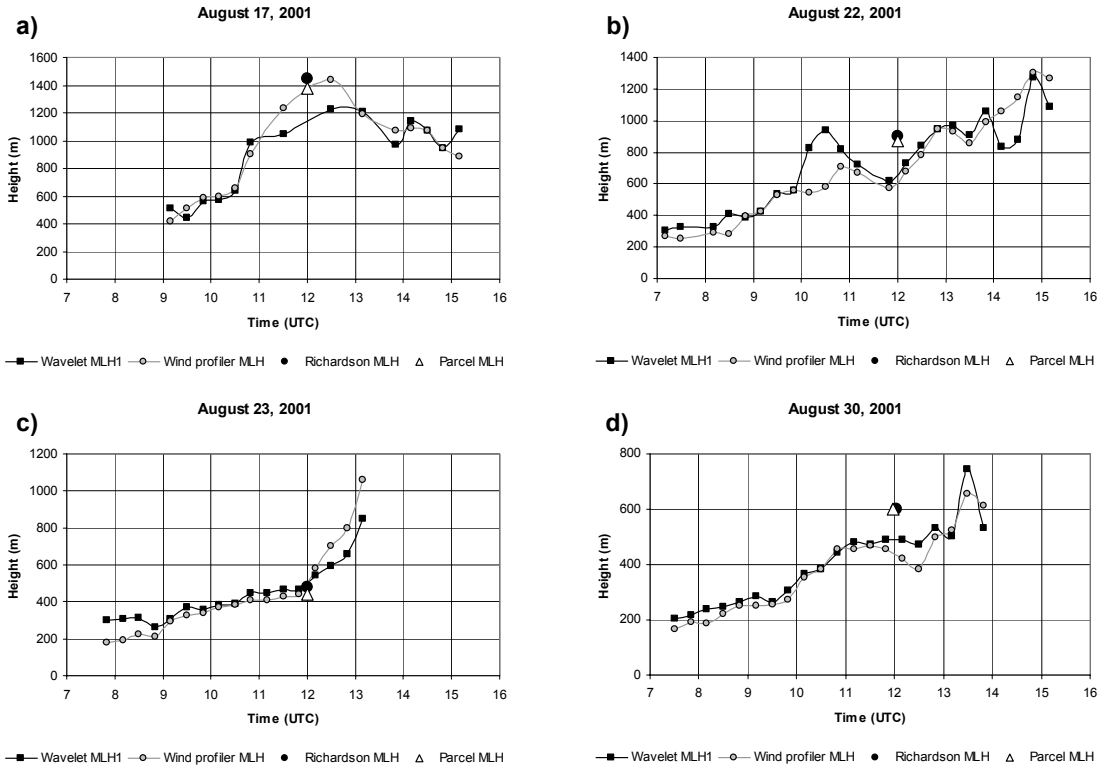

Fig. 8. Mixing layer height for the LD-40 vs. wind profiler comparison in Cabauw, for a) August 17, b) August 22, c) August 23 and d) August 30, 2001. Radiosonde estimates of MLH at 12 UTC are also shown.

The Wavelet MLH algorithm was applied to a data set of six years (2000-2005) of ceilometer data in De Bilt and Cabauw. The performance of the algorithm was analysed, leading to the following conclusions:

- The shape of the mean diurnal cycle of the MLH estimates shows the expected shape, but the afternoon values are significantly underestimated during spring and summer months. This is mainly caused by the limited range of the LD-40 in these months. This conclusion is supported by the frequency of occurrence distributions of LD-40 MLH estimates, which especially lack of values above 1250 m. Around 18 % of all 1961 cases analysed at 1200 UTC in the period 2000-2005 is affected by the limited vertical range of the LD-40 for MLH estimates. In these situations the SNR stop level is below the MLH as estimated by the Richardson bulk method applied to radiosonde profiles.
- The success rate for Wavelet MLH1 for all detections is between 43 and 68 % during the year. Highest success rates are found in summer, but this season also has the largest relative contribution of 'Weak' and 'Poor' detections. If only 'Good' detections of MLH are considered, the success rate is 20 to 30%.
- The overall agreement of LD-40 MLH and radiosonde MLH at 1200 UTC is poor. The main reason is that for high values of radiosonde MLH (i.e. above 500 m), the LD-40 MLH shows significantly lower values. This is again primarily caused by the limited vertical range of the ceilometer in spring and summer. The value for R^2 increases from 0.34 to 0.64 if only the 'Good' detections of Wavelet MLH1 are considered.
- A comparison with wind profiler estimates of the MLH in Cabauw (8 days) shows good agreement with a correlation coefficient R^2 of 0.89. The scatter increases for higher values of ceilometer MLH (> 500m).
- The MLH frequency of occurrence histograms of the RIVM lidar in Bilthoven demonstrate evident differences with the MLH histograms from the ceilometer algorithm. Much more high MLHs are found, particularly for the summer daytime detections. The comparison between the two algorithms is difficult, e.g. because the RIVM algorithm has the ability to estimate MLH in or above cloud layers, whereas the

LD-40 algorithm is terminated at the height of the first cloud base. The differences between the MLH histograms as derived from the LD-40 and RIVM algorithms are still under investigation.

- The users of the LD-40 MLH product should use the MLH estimates with care. The quality index can be used as a first check on the reliability. Furthermore, a visual inspection of variability of the MLH time series provides useful information.
- Improvements could probably be made after analysis of backscatter data in the raw Vaisala format, which may deliver more detailed information about the overlap correction and the backscatter profile in the lowest 150 m (Schäfer et al., 2004). Another possibility for improvement is to adapt the numerical resolution and range in the LD-40 data format used at KNMI.

ACKNOWLEDGEMENTS

The authors thank Christoph Münkel (Vaisala, for all the support on the LD-40 sensor, data formats and overlap issues), and Arnoud Apituley (RIVM, for the support on the RIVM MLH algorithm and providing the MLH time series from the research lidar in Bilthoven). The main part of the feasibility study was executed under contract of the BSIK ME2 project "Integrated observations and modeling of the greenhouse gas budget at a national level in The Netherlands".

REFERENCES

1. Brooks, I.M., 2003: Finding boundary layer top: application of a wavelet covariance transform to lidar backscatter profiles. *J. Atmos. Oceanic. Technol.*, **20**, pp. 1092-1105.
2. Cohn, S.A., and W.M Angevine, 2000: Boundary layer height and entrainment zone thickness measured by lidars and wind-profiling radars. *J. Appl. Meteorol.*, **39**, pp. 1233-1247.
3. Davis, K.J., N. Gamage, C.R. Hagelberg, C. Kiemle, D.H. Lenschow and P.P. Sullivan, 2000: An objective method for deriving atmospheric structure from airborne lidar observations. *J. Atmos. Oceanic. Technol.*, **17**, pp. 1455-1468.
4. Fischer, B.E.A., J.J. Erbrink, S. Finardi, P. Jeannet, S. Joffre, M.G. Morselli, U. Pechinger, P. Seibert and D.J. Thomson (Eds.), 1998: COST Action 710-Final Report. Harmonisation of the pre-processing of meteorological data for atmospheric dispersion models. L-2985 European Commission, Luxemburg. EUR 18195 EN (ISBN 92-828-3302-X).
5. Haij, de, M.J., H. Klein Baltink and W.M.F. Wauben, 2006: Description and evaluation of mixing layer height determination using a LD-40 ceilometer, *KNMI scientific report*, in preparation, De Bilt, The Netherlands.
6. Hutjes, R.W.A., 2005: Integrated observations and modeling of Greenhouse Gas budgets at the national level in The Netherlands. *Project proposal BSIK ME2 project*, Wageningen, The Netherlands.
7. Impulsphysik, 1998: User manual for laser ceilograph LD-25/40 Explorer/Tropopauser. Jenoptik Impulsphysik GmbH, Schenefeld, Germany.
8. Impulsphysik, 1999: Supplement 1 to User manual for laser ceilograph LD-25/40 Explorer/Tropopauser. Software Version V 3.4 15.12.1999 or higher. Jenoptik Impulsphysik GmbH, Schenefeld, Germany.
9. Menut, L., C. Flamant, J. Pelon and P.H. Flamant, 1999: Urban boundary layer height determination from lidar measurements over the Paris area. *Appl. Opt.*, **38**, pp. 945-954.
10. Münkel, C. and J. Räsänen, 2004: New optical concept for commercial lidar ceilometers scanning the boundary layer. *Remote Sensing of Clouds and the Atmosphere IX, Proceedings of SPIE, Bellingham, WA, USA*, **Vol. 5571**, pp. 364-374.
11. Pul, van, W.A.J., A.A.M. Holtslag and D.P.J. Swart, 1994: A comparison of ABL heights inferred routinely from lidar and radiosondes at noontime. *Boundary-Layer Meteorol*, **68**, pp 173-191.
12. Ruiter, de, A., 1991: Automatische menghoogtebepaling met lidar. *M. Sc. Thesis University of Amsterdam*, Amsterdam, The Netherlands.
13. Schäfer, K., S. Emeis, A. Rauch, C. Münkel and S. Vogt, 2004: Determination of mixing layer heights from ceilometer data. *Remote Sensing of Clouds and the Atmosphere IX, Proceedings of SPIE, Bellingham, WA, USA*, **Vol. 5571**, pp. 248-259.
14. Troen, I. and L. Mahrt, 1986: A simple model of the planetary boundary layer: Sensitivity to surface evaporation. *Boundary-Layer Meteorol*, **37**, pp 129-148.